

RSC Advances



This is an *Accepted Manuscript*, which has been through the Royal Society of Chemistry peer review process and has been accepted for publication.

Accepted Manuscripts are published online shortly after acceptance, before technical editing, formatting and proof reading. Using this free service, authors can make their results available to the community, in citable form, before we publish the edited article. This *Accepted Manuscript* will be replaced by the edited, formatted and paginated article as soon as this is available.

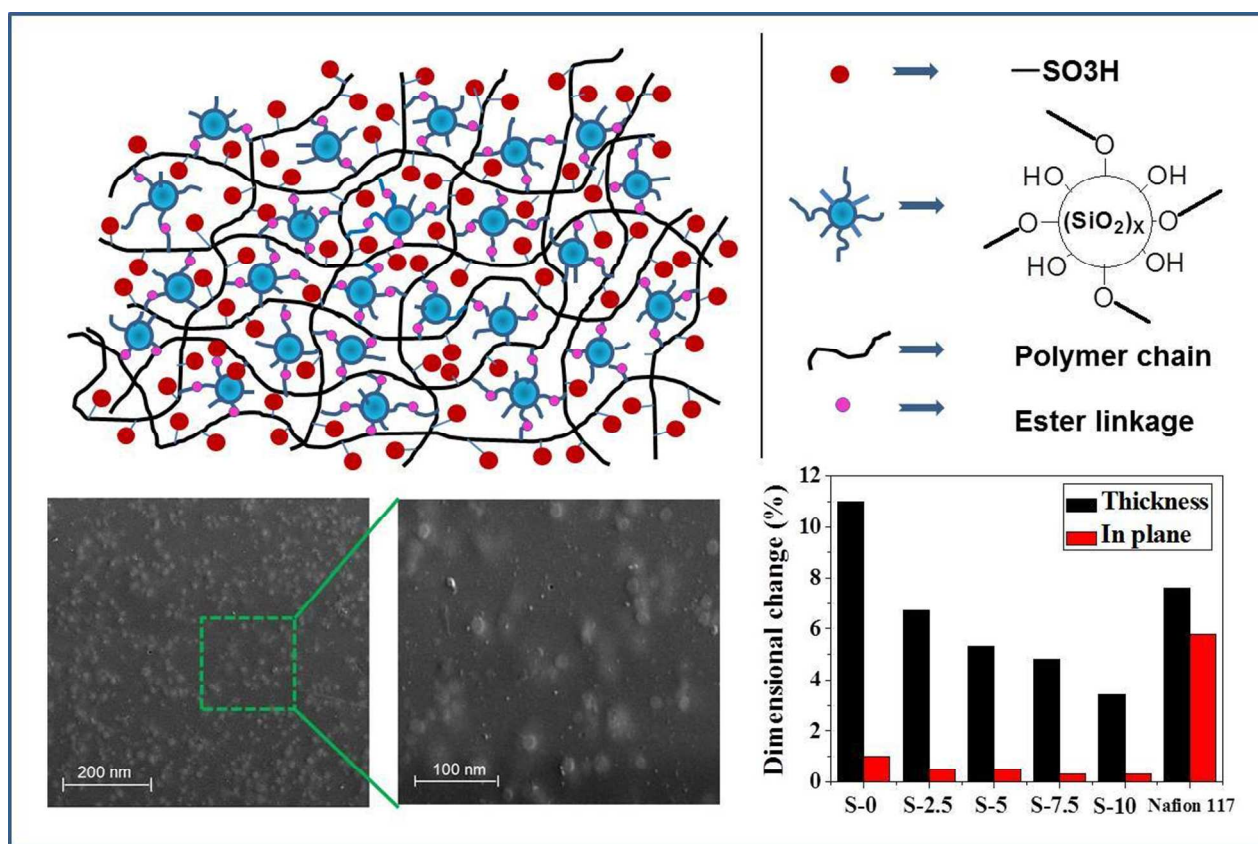
You can find more information about *Accepted Manuscripts* in the [Information for Authors](#).

Please note that technical editing may introduce minor changes to the text and/or graphics, which may alter content. The journal's standard [Terms & Conditions](#) and the [Ethical guidelines](#) still apply. In no event shall the Royal Society of Chemistry be held responsible for any errors or omissions in this *Accepted Manuscript* or any consequences arising from the use of any information it contains.

Graphical Abstract:

Cross-linked Sulfonated Poly(ether imide)/silica Organic–inorganic Hybrid Materials: Proton Exchange Membrane Properties

Ershad Ali Mistri, Susanta Banerjee*



Highlights: Hybrid proton exchange membrane with enhanced oxidative and dimensional stability as well as reduced fuel crossover.

Cross-linked Sulfonated Poly(ether imide)/silica Organic–inorganic Hybrid Materials: Proton Exchange Membrane Properties

Ershad Ali Mistri, Susanta Banerjee*

Materials Science Centre, Indian Institute of Technology Kharagpur,

Kharagpur-721302, India

RSC Advances Accepted Manuscript

Abstract

A series of sulfonated poly(ether imide)–silica hybrid membranes (SPI/S-X) were prepared from fluorine-containing ter-copolyimide and ~15 nm colloidal silica particles. The soluble poly(ether imide) with carboxylic acid pendant groups was synthesized by one pot high temperature polycondensation reaction using a sulfonated diamine, 4,4'-diaminostilbene-2,2'-disulfonic acid (DSDSA), fluorinated quadri diamine (QA), 3,5-diaminobenzoic acid (DABA) and 1,4,5,8-naphthalenetetracarboxylic dianhydride (NTDA). Such pendant carboxylic acid groups undergo condensation reaction with colloidal silica to provide organic–inorganic bonding that effectively improves the compatibility of nanocomposite membranes. Structure of the synthesized polymer was analysed by FT-IR and ¹H NMR spectroscopy. The esterification reaction was carried out between colloidal silica particles (with different loading) and the carboxylic acid containing polymer chains by thermal treatment in presence of *p*-toluenesulfonic acid (PTSA), which catalysed the esterification reaction. The prepared hybrid membranes exhibited excellent thermal and oxidative stability. Mechanical properties of the membranes were enhanced with certain wt. % of silica loading whereas the swelling ratio and oxygen permeability of the membranes was reduced by cross-linking. The microstructure of the resulting hybrid membranes were extensively investigated by SEM and TEM. Good compatibility and uniform distribution of the silica nanoparticles in the hybrid membrane was observed by SEM. Excellent nano-phase separated structure was observed under TEM which indicated the formation of well-dispersed hydrophilic domains throughout the membrane. The hybrid membranes showed significantly high proton conductivity in water medium which is in the range of commercially available Nafion[®] membrane under similar experimental condition.

* Corresponding author: Tel.: +91-3222-283972; fax: +91-3222-255303.
E-mail address: susanta@matssc.iitkgp.ernet.in (S. Banerjee)

■ Introduction

Presently, development of new polymers for proton-exchange membrane fuel cells (PEMFCs) has become a very active research area for both mobile and stationary applications. Compared to other energy converting devices, PEMFCs are considered as one of the most promising clean energy conversion technologies to address the environmental issues caused by the use of fossil fuels.¹ Thus, there is a great demand for durable proton exchange membranes (PEMs) with optimum physical properties along with high proton conductivity. PEM plays a major role as a proton conductor and separator of the hydrogen fuel from the oxidant in PEMFCs. The current state-of-the-art PEMFC technology relies on perfluorosulfonic acid (PFSA) membranes, such as Nafion[®].² However, Nafion[®] typically show certain drawbacks such as high cost, high fuel crossover, and restricted temperature (≤ 80 °C) operating conditions which prevent its widespread use in PEMFCs.^{3,4} In this respect, much research effort is being directed to develop new PEMs with lower cost and good overall performance as alternatives to replace perfluorosulfonic acid type membranes.

During past few years, numerous series of sulfonated aromatic copolymers based on poly(arylene sulfone)s,^{5,6} poly(arylene ether)s,^{7,8,9} polybenzimidazoles,^{10,11} polyimides,¹²⁻¹⁴ etc. have been widely studied as promising candidates for the next-generation PEMs. Aromatic sulfonated polyimides (SPIs) have received widespread interest as PEMs, because of their excellent heat resistance, chemical stability, mechanical strength, excellent film-forming ability, strong resistance to fuel crossover and high proton conductivity.¹²⁻¹⁴ The structure of SPI can be designed by using suitable monomers and/or by introducing suitable functional groups to the polymer backbone, so that the property of the membrane can be alternated correspondingly. Many research groups extensively studied SPIs as PEMs and they obtained lots of valuable results. Few reports from the literature described that SPIs containing flexible ether linkages

exhibited much better chemical and dimensional stability.^{13,15} Ameduri et al. reported that, incorporation of fluorine atom into the polymer backbone play an important role for the improvement of thermal, mechanical, chemical and oxidizing stabilities of the resulting fuel cell membranes.¹⁶ It is also known that the trifluoromethyl substituents are effective in improving the solubility and oxidation stability of SPI membranes.¹⁷ However, except few, all the reported sulfonated polymers suffer from the same drawback of poor hydrolytic-oxidative and dimensional stability in relatively high sulfonation content. Also, at high sulfonation content, the membrane swelling increases due to high water uptake (WU) and hence the mechanical property deteriorates. On the contrary, high degree of sulfonation (DS) is required for the SPI membrane to have higher proton conductivity.

Various approaches like semi-interpenetrating polymer networks, organic– inorganic hybrid, nanocomposite and cross-linking and so on have been adopted to improve the oxidative stability, dimensional stability, thermo-mechanical stability, water retention capacity and proton conductivity of the membranes.¹⁸⁻²⁰ One possible solution of the problem is crosslinking approach. Although cross-linking is a useful means to decrease the swelling ratio and limit fuel-crossover, it exhibits a little loss in proton conductivity and complication in the post-treatment. Park et al. reported crosslinked SPI through DABA containing monomer by using different aliphatic diols as crosslinkers and studied the effect of aliphatic chain length on PEM properties.²¹ They found improved properties for crosslinked SPI membranes with little sacrifice of proton conductivity, when the aliphatic chain length ≤ 4 . Another approach to introduce cross-linking structure is organic–inorganic hybrids. The advantage of this method is that the water retention, proton conductivity, thermo-oxidative stability of the membranes, which depend strongly on the dispersed state of the inorganic particles and the interfacial adhesion between organic–inorganic phases, can be improved by the organic–inorganic cross-linking structure.

Now, among many hydrophilic inorganic components, silica nanoparticles are considered as one of the most promising material for preparation of hybrid organic–inorganic polymer electrolyte membranes.²² The hydrophilic silica nanoparticles have numerous silanol (Si–OH) groups on their surface which might enhance water retention and therefore proton transport at low relative humidity (RH). Optimal introduction of such silica nanoparticles into SPI polymer matrix is a significant approach to improve desired membrane properties to be used as PEM material for fuel cell. Commonly, sol-gel method can be used to prepare SPI-silica hybrid materials by taking a silica precursor like tetraethylorthosilicate (TEOS) and poly(amic acid). However, there is a compatibility issue between SPI and silica by using this method which restricts the silica particles to disperse uniformly into the polymer matrix and the hybrid materials thus become opaque with increase in silica content. This is because of rapid agglomeration of silica particles which took place with the increase in the silica content within the SPI–silica hybrid materials prepared via the sol-gel method. Hence, improvements in the compatibility between the organic-inorganic phases, as well as reductions in silica particle size, have been realized in the preparation of SPI–silica hybrid materials. In this context, SPI interpenetrating polymer network (IPN)–silica nanocomposite membranes were fabricated by Lee et al.²³ where, a synthetic surfactant, urethane acrylate non-ionomer (UAN) has been used as a dispersant to homogeneously distribute silica nanoparticles as well as an IPN-type crosslinker.

We report chemical crosslinking between silica and polymer backbone by esterification method to prepare the hybrid membranes, without using any synthetic surfactant or, coupling agent. Hydrophilic colloidal silica (av. size ~15 nm) was used as a crosslinker so that an organic-inorganic bond can be formed through the surface silanol groups, which not only helps for the uniform dispersion of silica nanoparticles into the polymer matrix but also boost the synergistic effect on macroscopic composite-type PEM properties such as the thermal, mechanical, chemical

and dimensional stability. Moreover, during crosslinking process we are able to restrict the crosslinking solely to the free –COOH group in presence of sulfonic acid group.²¹ Structure of the SPI polymer matrix was specifically designed by introducing flexible ether linkages and trifluoromethyl substituents to have better performance of the electrolyte membrane. The carboxylic acid groups in the SPI copolymer was introduced by using DABA as a co-monomer which could act as an active pendant group for condensation reaction with the silanol groups of colloidal silica to provide organic-inorganic covalent bonding. Fabrication of hybrid nanocomposite was carried out by widely acceptable solution mixing technique to have uniform dispersion of silica nanoparticles within the polymer matrix followed by post etherification during membrane formation stage. The chemical structure and the morphologies of the membranes were examined by FT-IR, ¹H NMR, SEM and TEM techniques. Also, the physico-chemical and PEM properties of these hybrid membranes were thoroughly investigated to understand the effect of silica content and cross-linking network structure.

■ Experimental section

Materials. 1,4,5,8-Naphthalenetetracarboxylic dianhydride (NTDA) {Sigma-Aldrich (USA)} and 4,4'-diaminostilbene-2,2'-disulfonic acid (DSDSA) {Alfa Aesar (UK)} were dried in a vacuum oven at 120 °C overnight prior to use. Detailed synthesis of 4,4-bis[3'-trifluoromethyl-4'(4-aminobenzoxy)benzyl] biphenyl (QA) has been reported in our previous article.²⁴ 3, 5-Diaminobenzoic acid (DABA) {Aldrich (USA)}, PTSA (Rankem, India) and colloidal silica (Chemiewerk, 30 wt%, 15 nm) were used as received. Triethylamine (TEA, 99.0%), m-cresol (99.0%), dimethyl sulfoxide (DMSO) and benzoic acid (>99.5%) were purchased from E. Merck (India) and were used as received. Nafion[®] 117 was used in this study as the control membrane and was obtained from Alfa Aesar (UK).

Synthesis of Sulfonated Poly(ether imide) with Reactive Carboxyl Groups (DQDN-70). In a 100 mL 3-necked flask equipped with a magnetic stirrer and N₂ inlet, 1.2192 g (3.29 mmol) DSDSA, 20 mL m-cresol and 0.92 mL (6.58 mmol) TEA (density 0.72 g/mL) were added. The mixture was heated to 80 °C and was stirred under N₂ flow until DSDSA was completely dissolved. To it, 0.6175 g (0.94 mmol) QA, 0.0715 g (0.47 mmol) DABA, 1.2611 g (4.70 mmol) NTDA and 1.1485 g benzoic acid were added successively followed by the addition of 5 mL m-cresol. The mixture was stirred at 80 °C for 4 hours, at 180 °C for 16 hours and at 195 °C for 3 hours, respectively. After cooling to 80 °C, 15-20 mL m-cresol was added to dilute the highly viscous solution. Then the viscous polymer solution was slowly poured into excess acetone under constant stirring. The fibrous precipitate was collected by filtration and thoroughly washed with acetone followed by methanol to remove any residual solvent. Finally, fiber-like copolymer was collected after drying overnight at 120 °C under vacuum. ¹H NMR (DMSO-d₆): 8.8-8.7 (3, several signals due to different NDI-centred triads), 8.25 (26), 8.15 (27,29), 8.11 (11,13), 7.91 (24), 7.89 (16,17,21), 7.54 (6), 7.50 (25), 7.30 (14), 7.28 ppm (7). FT-IR (cm⁻¹): 1712, 1665 (C=O), 1345 (C-N), 1100, 1020 (SO₃H).

Fabrication of SPI/silica Hybrid Membranes. To prepare a series of hybrid SPI/silica membranes, at first a measured amount of the synthesized sulfonated poly (ether imide) in TEA salt form was dissolved in a round bottomed flask by using DMSO [5% (w/v)] as solvent. Then calculated amount of silica sol was added to it with vigorous stirring. By adjusting the amount of the silica sol to the SPI solution, different SPI/S-X hybrid systems with 2.5 wt.%, 5 wt.%, 7.5 wt.% and 10 wt.% of nano SiO₂ in DMSO were obtained. All the polymer solution containing silica sol was sonicated at least 20 minutes to ensure homogenous distribution. The esterification reaction was carried out at 140 °C for ~16h in DMSO with 5 mg of *p*-toluene sulfonic acid per gram of polymer for catalysis.

Different hybrid membranes were prepared by casting the corresponding DMSO solution onto Petri dishes and dried at 100 °C for 12 h for slow removal of the solvent, then the temperature was slowly raised to 120 °C, 140 °C and 160 °C each for 2 h. Finally, the samples were heated at 180 °C for 7-8 h to complete crosslinking. The prepared hybrid membranes are termed as SPI/S-X (X represents the theoretical amount in wt.% of silica in the hybrid membrane). The pristine SPI (designated as SPI/S-0) was prepared without PTSA. After cooling down to room temperature the membranes were peeled off from the Petri dishes by dipping them in water. Next the membranes were soaked in methanol at 60 °C for 1 h to remove any residual solvents. The hybrid membranes along with the pristine SPI membrane were converted to the required acid form by immersion in the 1.5 M sulphuric acid solution at room temperature for 48 h followed by washing with deionized (DI) water several times until it reached neutral pH. Thereafter, all the membranes were dried in vacuum oven at 120 °C for overnight. The thickness of the membranes was in the range of 40-50 μm ($\pm 1 \mu\text{m}$).

Measurements and Characterization Methods. $^1\text{H-NMR}$ spectrum of the copolymer was recorded on a Bruker 400 MHz NMR Spectrometer using DMSO- d_6 as solvent and tetramethylsilane (TMS) as reference. ATR-FTIR spectra of the hybrid membranes as well as pristine membrane were recorded from a NEXUS 870 FTIR (Thermo Nicolet) spectrophotometer at room temperature. The inherent viscosity was determined on 0.5 g dL^{-1} concentration of the pristine copolymer in DMSO with an Ubbelohde capillary viscometer at 30 °C. Thermo-gravimetric analysis (TGA) was conducted utilizing a Perkin Elmer Pyris Diamond TG-DTA thermo-gravimetric analyzer by heating the samples from ambient temperature to 700 °C with a heating rate of 10 °C min^{-1} under synthetic air ($\text{N}_2:\text{O}_2$ is 80:20). Stress-strain behavior of the wet membranes ($10 \times 25 \text{ mm}^2$) was measured at room temperature using Universal Testing Machine (UTM)-Instron, Plus-8800 at a cross-head speed of 5% min^{-1} of the specimen

length. Transmission electron microscopy (TEM) of ultra-microtome membranes was carried out using a FEI - TECNAI G2 20S – TWIN microscope (USA) with acceleration voltage of 100 kV. In order to stain the ionic domains, membrane samples in acid form were converted into Ag^+ form by immersing them in 0.5 M AgNO_3 aqueous solution overnight. The samples were thoroughly rinsed with deionised water and dried at room temperature for 24 h before measurement. Thin slices (200 nm) of the embedded membranes were cut using an ultra-microtome fitted with a diamond knife and were transferred onto carbon-coated copper grids for TEM analysis. The surface morphologies of the membranes were examined with a ZEISS EVO 60 (Carl ZEISS SMT, Germany) scanning electron microscope (SEM) equipped with Oxford energy-dispersive X-ray spectroscopy (EDS) detector. All the hybrid membranes were vacuum sputtered with a thin layer of Au prior to SEM examination.

The ion contents of the membranes were represented by ion exchange capacity (IEC). The calculated IEC values are theoretically calculated from the amount of sulfonic acid groups and carboxylic acid groups in the copolymer and the measured IEC values were determined by classical titration method. The measured IEC_{Titr} , WU and the hydration number (λ) of the membranes were determined according to our reported article.¹⁴ Dimensional change in membrane thickness (Δt) and length (Δl) were measured by immersing more than two samples in water at 30 °C for 24 h. The changes of thickness and length were calculated from:

$$\Delta t = (t_s - t_d) / t_d$$

$$\Delta l = (l_s - l_d) / l_d$$

Where, t_d and l_d are the thickness and length of the dry membrane respectively, t_s and l_s refer to those of the membrane immersed in water.

The hydrolytic stability of the SPI/S-X membranes was investigated by comparing the IEC_{Titr} value before and after immersing them in pressurized water at 120 °C for 24 h. The

oxidative stability was determined by measuring the elapsed times at which the membranes dissolved completely into Fenton's reagent (3% H₂O₂, 2 ppm FeSO₄ solution) at 80 °C.¹² The proton conductivity (σ) in-plane direction^{14,25} of the membranes were examined using AC impedance spectroscopy (HIOKI 3532-50 LCR Hi Tester, Japan) over a frequency range of 100 Hz–2 MHz. Hydrated membrane of dimension (2 × 1) cm² was placed on two parallel platinum electrodes separated by 0.8 cm in the conductivity cell^{14,25} and was exposed to allow its equilibrium with DI water during the experiment. Proton conductivity of the membranes was determined according to the reported procedure.¹⁴ Furthermore; proton conductivity was also tested at 75% RH condition at room temperature to examine the effect of silica loading on proton transport at relatively lower humidity.

The oxygen permeability coefficients²⁶ was measured at 3.5 bar of applied gas pressure and at 35 °C using automated Diffusion Permeameter (DP-100-A) manufactured by Porous Materials Inc., USA. The permeability coefficients are reported in barrer and were calculated from:

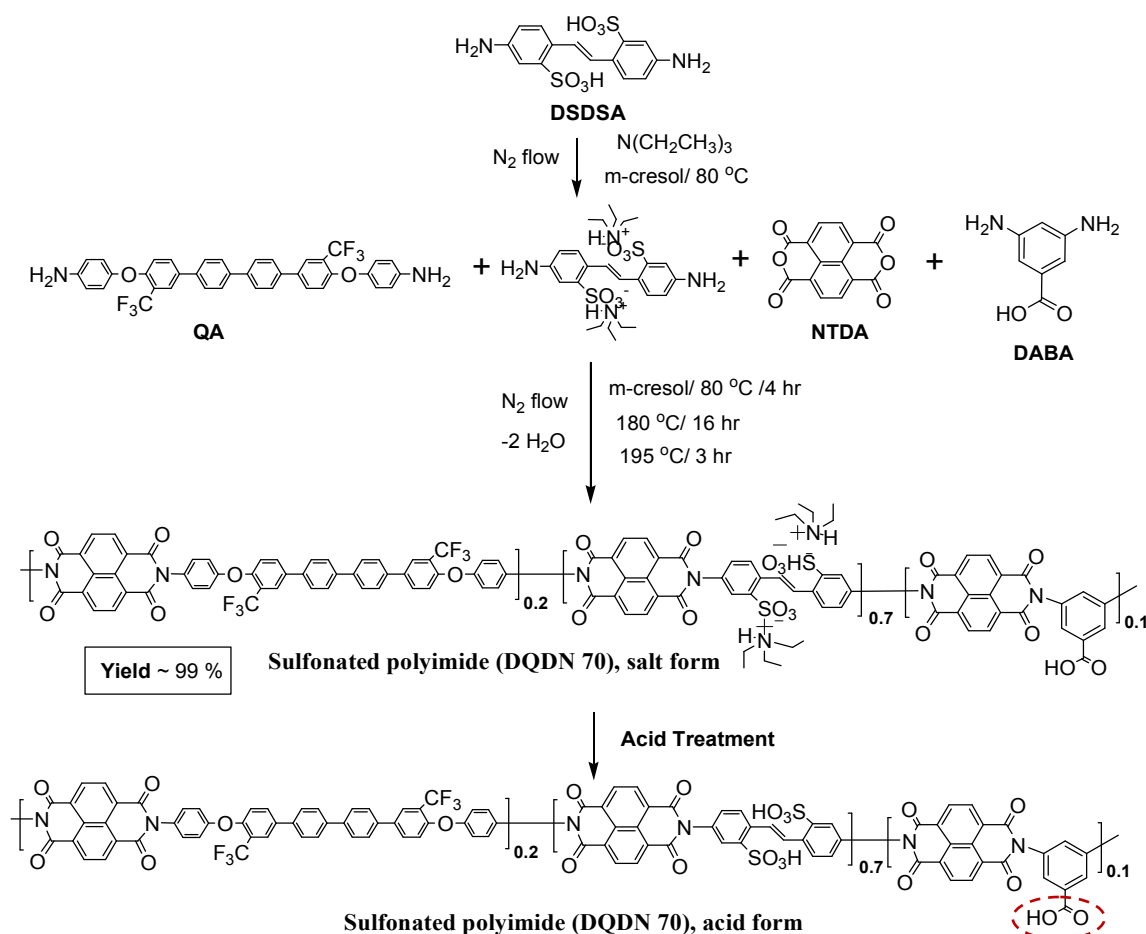
$$P = [VdT_0/Ap_i p_0T] (dp/dt)_s$$

Where, T_0 and p_0 are the standard temperature and pressure ($T_0 = 273.15$ K, $p_0 = 1.026$ bar), T is the temperature of measurement, d is the thickness of the membrane and $(dp/dt)_s$ was obtained from the slope of the increments of downstream pressure vs. time plot.

■ Results and discussion

Synthesis and Characterization of the Polymer. In order to prepare the sulfonated poly(ether imide) containing active carboxyl groups, DABA was chosen as a co-monomer along with DSDSA and QA. These three diamine monomer were reacted with a six-membered dianhydride, NTDA through one-pot high temperature poly-condensation reaction in m-cresol solvent in the presence of TEA and benzoic acid. In this preparation, stoichiometric amount of

TEA was added to the DSDSA solution which not only helps to solubilize the sulfonated diamine monomer, but also produced the free much more reactive non-zwitterion diamine groups for imidization reaction.^{13,14} A schematic representation for synthesis of the ter-copolymer, DQDN-70 is shown in **Scheme 1**. The synthesized copolymer had 70 mol% disulfonated units and 10 mol% carboxylic acid groups in the polymer backbone. The inherent viscosity of the synthesized copolymer, DQDN-70 was evaluated from its solution in DMSO (0.5 g/dL), and value was found as 1.35 dL/g. High viscosity value of the copolymer indicated the formation of high molar mass. The chemical structure of the copolymer, DQDN-70 was confirmed by ¹H-NMR spectroscopy.



Scheme 1. Synthetic procedure of fluorine-containing SPI with reactive carboxyl groups

As shown in **Figure 1**, the $^1\text{H-NMR}$ spectrum of the SPI copolymer DQDN-70 in DMSO-d_6 depict signals of aromatic protons in the range of 7–9 ppm, all of which were assigned to the proposed repeat unit structure within acceptable integral values corresponds to magnetically different protons. The detail NMR analysis of similar kind of copolymer structure has been described in our previous article.¹⁴ The additional signal for 10 mol% DABA unit came at around 8.15 ppm (H_{27} , H_{29}), which combined with the peak of H_{11} and H_{13} . However, the signal corresponds to acidic proton was not observed. This could be due to low mol% DABA in polymer repeat unit. To further confirm the incorporation DABA in the polymer repeat unit a model reaction with higher mol% of DABA was conducted (30 mol% DABA and 70 mol% DSDSA). The polymer was characterized and $^1\text{H-NMR}$ spectrum of which showed the presence of free carboxylic acid group (acidic proton at 13.35 ppm) (See ESI, Figure S1). Hence, during the polymerization reaction, all diamine monomers get reacted to more reactive dianhydride leaving free carboxylic acid group.

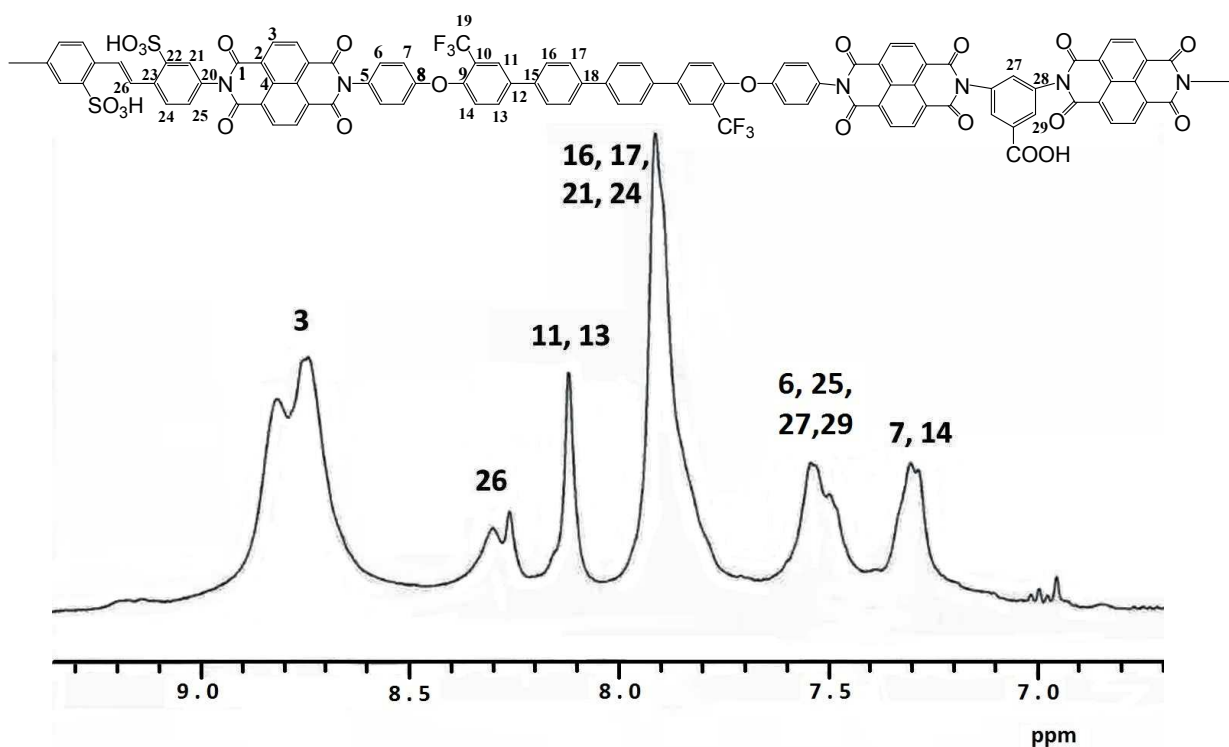


Figure 1. $^1\text{H-NMR}$ spectrum of DQDN-70 copolymer with signal assignment

Fabrication of SPI/S-X Hybrid Composite Membranes. Hybridization between organic and inorganic segments was carried out at the molecular level by covalent bonding that effectively improves the compatibility of this reported nanocomposite polyelectrolyte membrane. Esterification reaction was took place between the free carboxyl groups of the ter-copolymer and the silanol ($-\text{Si}-\text{OH}$) groups of colloidal silica particles by thermal treatment in the presence of PTSA catalyst. Crosslinking was restricted solely to the free $-\text{COOH}$ group as the sulfonic acid group was in TEA salt form during this process. All the casted membranes in TEA salt form were converted to the required acid form according to the process described in the experimental section. Covalent crosslinking of DABA-containing SPI is presented in **Figure 2**. All the hybrid membranes were brown and flexible even when the SiO_2 content was up to 10 wt.%.

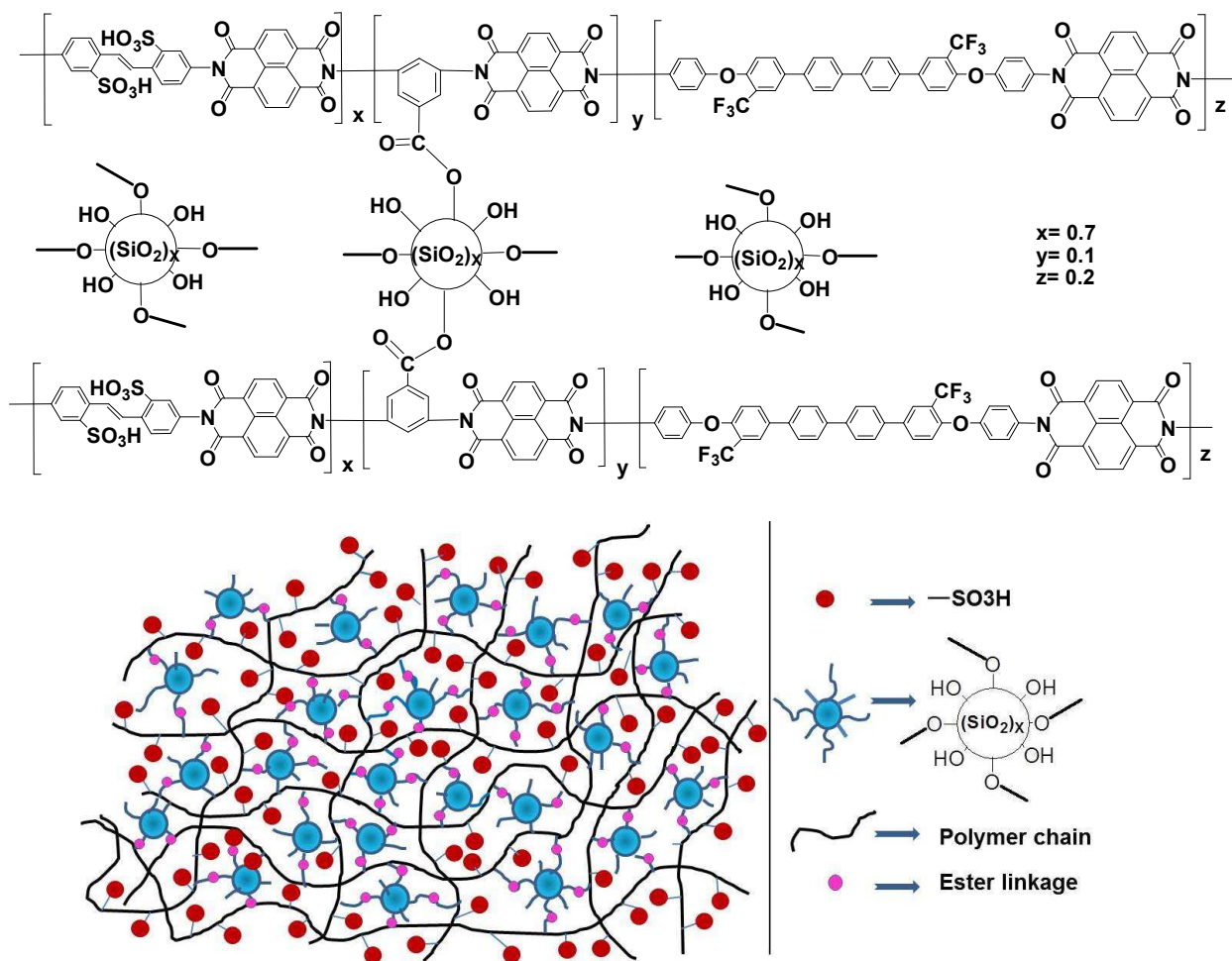
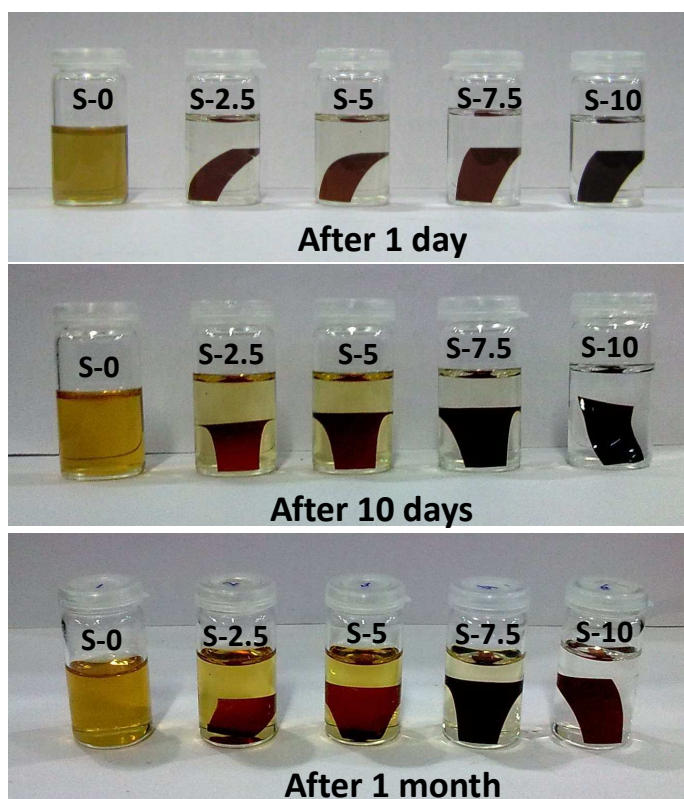


Figure 2. Cross-linked structure of SPI/silica hybrid membrane

The solubility of SPI/S-X hybrid composite membranes in polar aprotic solvents was significantly low, whereas the pristine SPI membrane exhibited good solubility in polar aprotic solvents like DMSO, dimethylacetamide (DMAc) or, dimethyl formamide (DMF). For example, SPI/S-X hybrid membranes did not dissolve in DMAc, even after months, while the pristine SPI membrane dissolved in overnight (**Figure 3**). This suggested that silica particles have been successfully undergoes covalent cross-linking which enhances the membranes stability in solvents.

**Figure 3.** Solubility of SPI/S-X membranes in DMAc solvent

The formation of SPI and presence of silica were verified by FTIR spectra (provided in ESI, Figure S2) which showed absorption bands of naphthalene imide rings at about 1345 cm^{-1} (C–N asymmetric), 1665 cm^{-1} (C=O asymmetric) and 1712 cm^{-1} (C=O symmetric) which are

characteristic of six-membered imide ring¹⁴. SO₂ stretching vibration of the sulfonic acid group was observed as a broad band at around 1020 cm⁻¹ and 1100 cm⁻¹. The peak at 810 cm⁻¹ can be ascribed to the symmetric Si—O—Si_{str} vibration, which gradually increases and broadened with increase in silica content. Moreover, a broad absorption band in the region 1000-1100 cm⁻¹ arises due to asymmetric Si—O—Si_{str} vibration that comes from the incorporated silica of the hybrid membranes. However, one of the SO₂ stretching vibration of the sulfonic acid group was also arises in that region. It is noteworthy to mention that absorption band at around 1712 cm⁻¹ also represents the ester bond of crosslinked SPI/S-X membranes that overlaps with the symmetric imide C=O stretching, whose intensity increases with increase in silica content.²⁷ An energy dispersive spectrometry (EDS) experiment was also performed to verify the presence of silica in prepared hybrid membranes. EDS analysis confirmed the existence of Si in the membrane. A clear signal corresponds to silicon atom was present at 1.74 keV in the EDS spectrum of SPI/S-X hybrid membranes whereas there was no signal in the pristine SPI membrane (**Figure 4**).

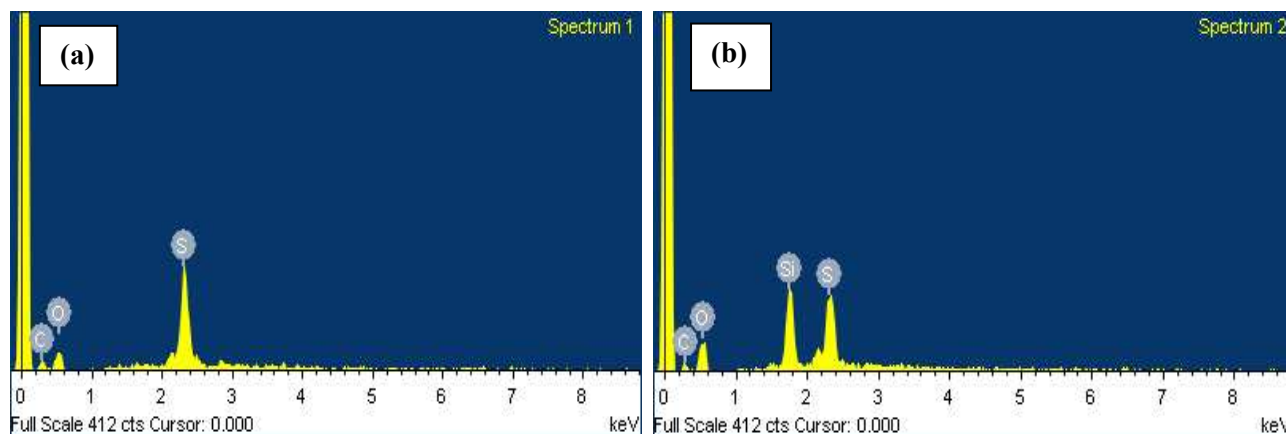


Figure 4. EDS spectra of (a) pristine SPI and (b) SPI/S-2.5

Thermal and Mechanical Properties. Thermal properties of the membranes were investigated by thermo gravimetric analysis (TGA) measurements. **Figure 5a** shows the thermal decomposition thermograms of the SPI/S-X membranes with different SiO₂ loading. Three

consecutive weight loss steps were observed in the thermograms which resulted from the processes of dehydration, thermal desulfonation and thermal oxidation of the polymer matrix.^{14,17} The initial weight loss at around 100 °C is associated with the loss of absorbed water within the membranes. The secondary weight loss which started from around 340 °C is due to the decomposition of sulfonic acid groups. Third weight loss started at around 480–500 °C corresponds to the pyrolysis of SPI backbone. Again, from the figure it is observed that third weight loss temperature which was started at around 480 °C for pristine SPI membrane shifted slightly towards higher temperature ~500 °C for the hybrid SPI/S-X membranes. This may take place due to the formation of SiO₂ network. The TGA results revealed that all the SPI/S-X membranes had fairly good thermal stability, where the onset of thermal decomposition of sulfonated moieties (~340 °C) occurred well above the servicing temperature (70 °C to 120 °C) for a PEM fuel cell application. In addition, the increase in weight residues at 700 °C suggests the successful incorporation of higher amount of silica into the hybrid membranes, which ultimately increases the thermal stability of membranes. The amount of SiO₂ residue measured was nearly proportional to the mass fraction of SiO₂ introduced during the casting procedure (**Figure 5b**). However, a mass residue was observed in the TGA thermo-gram of the pristine SPI, which may come from the impurities introduced during the film casting, or it may be graphitic-like carbon that formed through thermal pyrolysis.

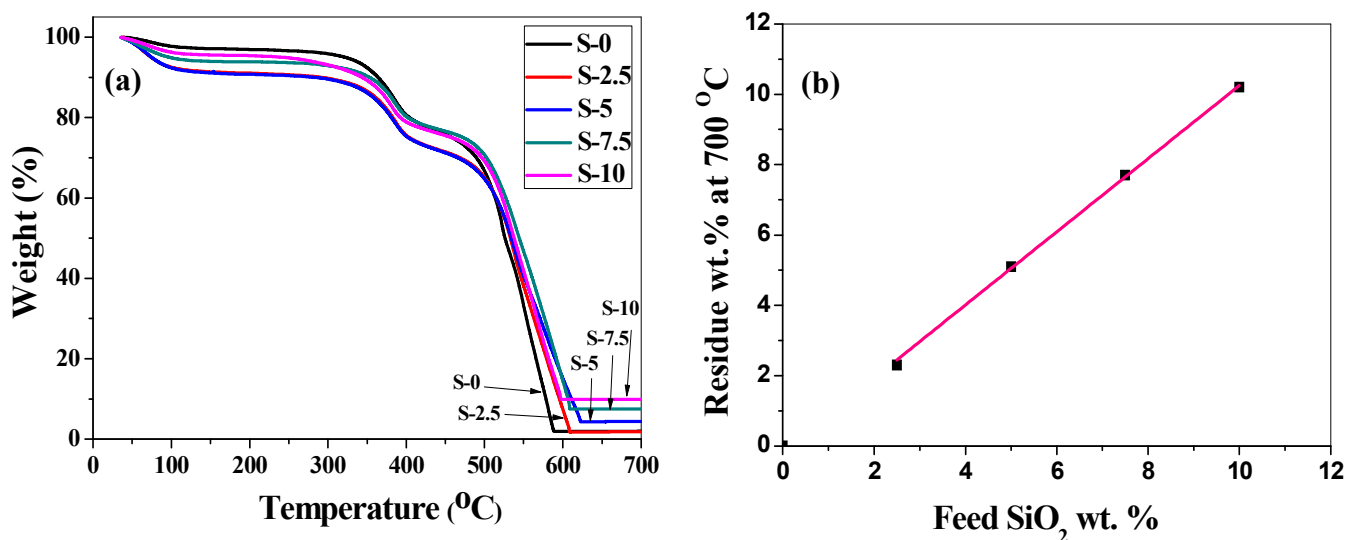


Figure 5. Thermogravimetric analysis of SPI/S-X hybrid membranes (a) thermograms of the representative samples; (b) correlation plot of SiO₂ feed versus residual mass in wt.%

It is essential for PEMs to possess adequate mechanical integrity in humidified condition to withstand the fabrication of the membrane electrode assembly. That is why the mechanical properties of all the SPI/S-X membranes were measured in hydrated state (membranes were immersed in DI water for 24 h at room temperature, taken out and wiped out with tissue paper prior to test) and the results are listed in **Table 1**. All the SPI-/S-X membrane possess good tensile strength (~57 to 95 MPa) and young modulus (2.23 to 2.92 GPa) in hydrated condition. From the stress-strain plot (ESI, Figure S3) it was observed that the incorporation of SiO₂ particles into the SPI matrix improves the tensile strength and Young's modulus of the membranes gradually up to certain SiO₂ content. The tensile strength and Young's modulus of the SPI/S-5 hybrid membrane increases 23.7% and 30.94% as compare to pristine SPI membrane. However, when the SiO₂ content exceeds 5 wt.%, the tensile strength and the elongation of the membranes both decrease. For high silica loading (>5%), the microstructure of membranes started to change due to the aggregation of silica nanoparticles in SPI matrix and this

will result in the decline of the mechanical properties. The elongation at break decreases with increase in SiO₂ content due to the cross-linking network that restricted the motion of the SPI chain segmental. These results indicated that up to 5% SiO₂ loading, the mechanical properties of the hybrid membranes were improved significantly.

Table 1. Mechanical properties of different hybrid membranes

Polymer membranes	Tensile strength (MPa)	Young's modulus (GPa)	Elongation at break (%)	Ref.
SPI/S-0	76.79	2.23	5.2	This study
SPI/S-2.5	86.9	2.64	4.7	This study
SPI/S-5	94.98	2.92	6.1	This study
SPI/S-7.5	70.75	2.51	3.9	This study
SPI/S-10	57.62	2.65	2.4	This study
DQN70	84.6	1.56	22.9	[14]
Nafion® 117	21.9	0.16	288	This study

Oxidative Stability, Hydrolytic Stability and Dimensional Change. Oxidative stability is one of the important factors for evaluating the life time of PEMs under harsh fuel cell conditions. Oxidative stability of the pristine membrane and hybrid membranes were examined by recording the elapsed time in which the membranes (1cm×1 cm) dissolved completely under occasional stirring after immersion into Fenton's reagent [3% aqueous (v/v) H₂O₂ solution containing 2 ppm FeSO₄] at 80 °C. As shown in **Table 2** all SPI/S-X hybrid membranes displayed excellent oxidative stability which is much better than that of similar kind of sulfonated copolymer membranes in the same experimental condition.^{12,13,28} It was also observed that oxidative stability of the composite membrane increases with increasing silica content. The reason for better oxidative stability of hybrid membranes is due to the covalent crosslinking between the silica particles and polymer chains which protects the exposure of hydrogen-containing terminal bonds from the free radical species (HO• and HOO•). Again, the hybrid membranes exhibited relatively lower water uptake values than pristine SPI membrane that also helps to reduce the

direct water contact to the polymer chain. As the cross-linked network structure increases with the silica content, it becomes harder for free radicals to attack the polymer chain.. Interestingly, the pristine SPI membrane exhibits slightly better oxidative stability than the similar kind of SPI membrane, DQN 70 having same DS that was reported in our previous article.¹⁴ This can be explain by the fact that, in the present pristine SPI, the extra aromatic —COOH group from the DABA unit undergoes extensive intermolecular H-bonding that protects the terminal bonds of SPI from attack by free radical species. The hydrolytic stability of SPI/S-X membranes was also evaluated by immersing them in pressurized water at 120 °C for 24 h. All the membranes showed no obvious changes in their appearance, weight and IEC_{Titr} values, indicating very good hydrolytic stability of the membranes.

Table 2. Oxidative stability and dimensional stability of SPI/S-X membranes

Membrane	Thickness (µm)	Oxidative stability ^a (h)	Dimensional change ^b		Ref.
			Δt	Δl	
SPI/S-0	40	18	0.110	0.01	This study
SPI/S-2.5	48	25.5	0.067	0.005	This study
SPI/S-5	49	41	0.053	0.005	This study
SPI/S-7.5	49	>48	0.048	0.003	This study
SPI/S-10	50	>48	0.034	0.003	This study
DQN70	45	9	0.110	0.02	[14]
Nafion® 117	180	>48	0.076	0.06	This study

^a Tests performed in Fenton's reagent at 80 °C. Reported values are the elapsed times in which the membranes dissolved completely.

^b Measured at 30 °C.

Dimensional change is also considered as an important parameter for electrolyte membranes to be operated in fuel cell. Generally, high DS is required for the SPI membranes to achieve high proton conductivity, but at high DS membranes undergoes undesirable dimensional changes and the membranes can become highly swollen that is unsuitable for practical application. **Figure 6**

compares the dimensional swelling ratio of SPI/S-X membranes and Nafion[®] 117 in the through-plane and in-plane direction at 30 °C. Almost all the SPI/S-X membranes exhibited lower swelling ratio than that of Nafion[®]. Furthermore, the membranes showed a general trend of the reduction in swelling ratio i.e. increase in dimensional stability with the increasing SiO₂ loading from 0 to 10 wt.% (**Table 2**). This is due to the cross-linking network structure, which increased the interaction of the polymer molecules and restricted the movement of polymer chains in the hybrid membranes. In addition, the fluorinated SPI displayed anisotropic membrane swelling with relatively lower dimensional change in plane (Δl) direction than in thickness (Δt).¹⁴

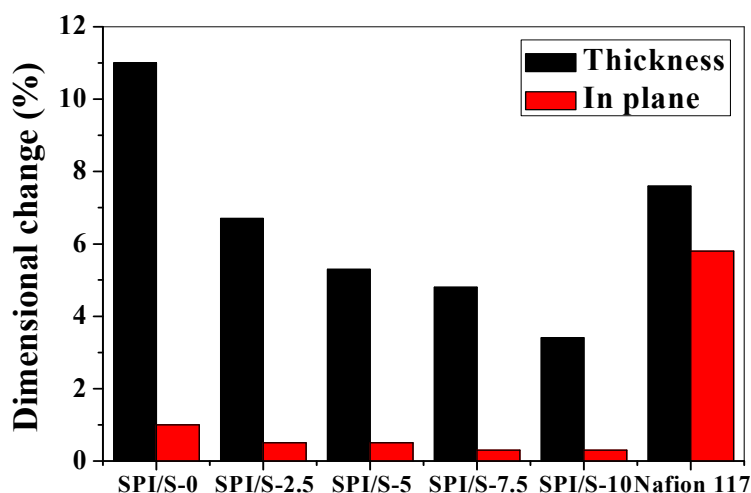


Figure 6. Dimensional swelling of SPI/S-X membranes and Nafion[®] 117 at 30 °C

Microstructure of the Membranes. The morphology of the membranes has been extensively studied by SEM and TEM techniques in order to understand the correlation between microstructure and membrane properties. The dispersion of silica nanoparticles into the organic polymer matrix was examined by SEM analysis. **Figure 7** shows the SEM micrograph of the hybrid membrane surface with different silica content. **Figure 7(a)** is an SEM image of the pristine SPI membrane surface, whereas **Figure 7(b)–(d)** shows the morphology of the hybrid

SPI/S-X membrane with 2.5%, 7.5% and 10% SiO₂ content, respectively. Uniform dispersion of SiO₂ particles in the SPI matrix was observed for all membranes. The covalent bond existed between SiO₂ particle and functionalized polymer facilitated better dispersion and improved the compatibility between the organic and inorganic components. It is also observed from the figure that the number density of SiO₂ particle on the membrane surface increases with gradual increase of SiO₂ content. However, the SPI/S-X hybrid membrane with 10 wt.% SiO₂ content shows relatively poor compatibility due to higher amount of silica content. For high SiO₂ content, the aggregation of SiO₂ particles becomes evident which can be observed from the **Figure 7(d)**. This phenomenon causes the decline of mechanical properties of the hybrid membrane.

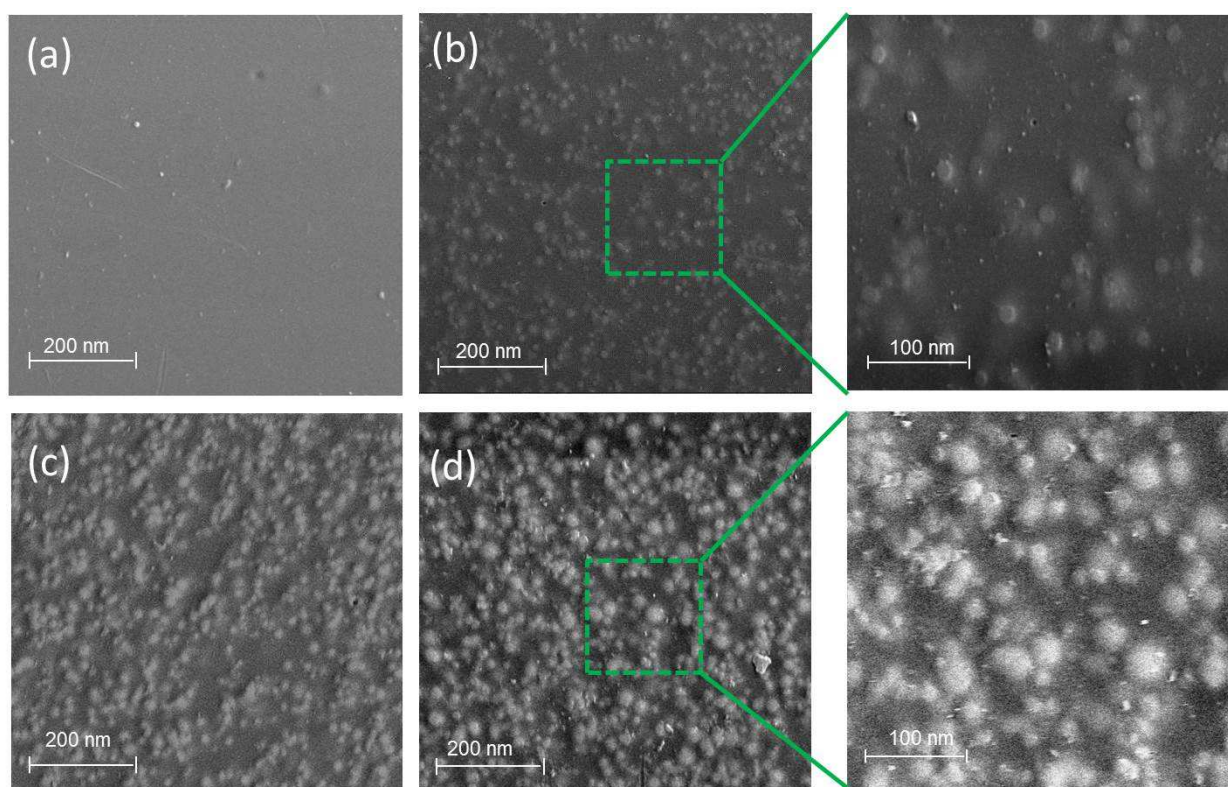


Figure 7. SEM images of the membrane surface with different SiO₂ contents (a) SPI/S-0; (b) SPI/S-2.5; (c) SPI/S-7.5; (d) SPI/S-10

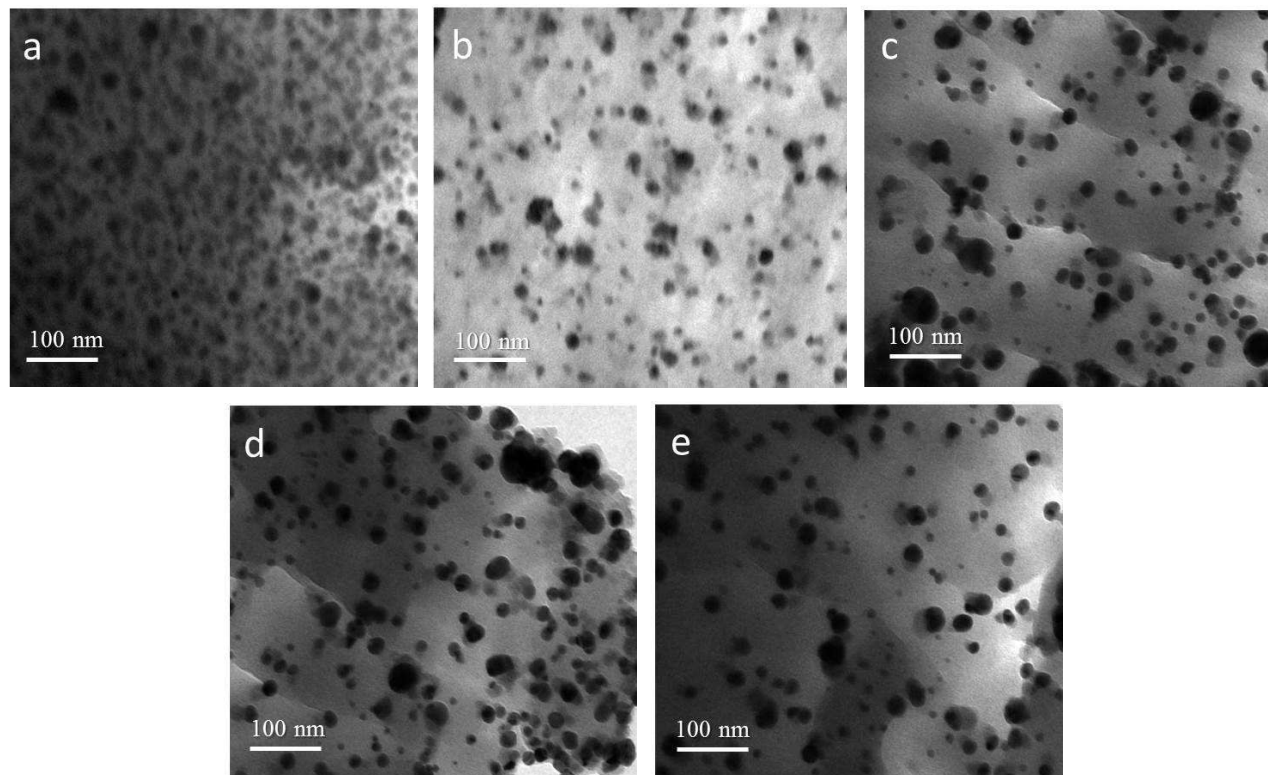


Figure 8. TEM images of SPI/S-X membranes (a) SPI/S-0; (b) SPI/S-2.5; (c) SPI/S-5; (d) SPI/S-7.5; (e) SPI/S-10 (cross section, in Ag⁺ form).

TEM analysis was carried out to investigate the bulk morphology of the SPI/S-X membranes, which plays an important role on proton transport. Firstly, to understand the nature and distribution of ionic domains (caused by sulfonate group) throughout the matrix, the membranes were stained by AgNO₃ solution. **Figure 8(a)–(e)** presents the cross-section

micrographs of the membranes which shows excellent phase separated morphology. The spherical darker regions indicate the hydrophilic ion clusters and the lighter area corresponds to hydrophobic non-ionic moieties.^{14,29} These hydrophilic clusters are mainly responsible for proton transport. It is noteworthy to mention that the size and number density of ionic clusters depends on the material's ionic content i.e. IEC.²⁹ It is observed from the figure that the size of the ionic cluster gradually increases with increasing silica content whereas the number density decreases at the same time. Such morphological trend arises may be due to the lowering of effective IEC of the SPI/S-X membranes with higher SiO₂ loading. Furthermore, TEM images of the colloidal SPI/silica solution in DMSO were examined for the case of SPI/S-5 and SPI/S-10 prior to thermal treatment (ESI, Figure S4). For SPI/S-5, homogenous distribution of SiO₂ nanoparticles with a particle size of ~15 nm was observed. However, in case of SPI/S-10 a non-homogenous distribution of SiO₂ nanoparticles was found and the nanoparticles were seems to aggregates.

IEC and Water uptake. IEC value is an important performance index of proton exchange membranes. Commonly, it represents the amount of exchangeable protons in ionomer membranes. The IEC values of SPI and their hybrid membranes are presented in **Table 3**. Calculated IEC values were theoretically calculated from the amount of sulfonic acid groups and carboxylic acid groups in the copolymer and the measured IEC values were obtained by titrimetric method. It was observed that the measured IEC values of hybrid SPI/S-X membranes decrease gradually from 2.29 mmol g⁻¹ to 1.93 mmol g⁻¹ with increasing SiO₂ content. The reduction of measured IEC values is associated with the dilution effect of SiO₂ particles and the consumption of free carboxylic acid groups in the copolymers by esterification reaction. The water molecules play a vital role in the proton exchange membrane and directly affect the proton transport across the membranes. There are two factors which controls the WU values of the hybrid membranes containing silica nanoparticles: (i) a hygroscopic effect due to the unreacted –

Si-OH group, which increase the content of bound water, (ii) SPI/silica cross-linked network structure which narrowed average inter-chain distance between polymer chains that reduces the free volume resulting limited absorbed water. As shown in **Table 3**, the WU value of the hybrid SPI/S-X membranes are lower than that of pristine SPI membrane and it gradually reduces with increasing of SiO₂ content. This can be explained by the fact that, the reduction of IEC value and free volume becomes the primary effecting factor on the WU as compared with the hygroscopic effect of the silica nanoparticles. This phenomenon is also supported by the microstructural analysis of the membranes. Water molecules per sulfonic acid group (λ) for the pristine polymer is found around 6, which is reduced with increasing in silica content due to crosslinking network structure that reduce the free volume to occupy water molecules around -SO₃H groups. However, up to SPI/S-7.5 i.e. up to 7.5 wt.% silica loading $\lambda \sim 4$ which is considered enough for smooth transportation of protons via vehicular mechanism.³⁰ The λ value for Nafion[®] 117 membrane ($\lambda \sim 10.8$) was found higher than that of SPI/S-X membranes. This is probably due to the higher rigidity of the aromatic SPI backbone containing quadriphenyl moiety and crosslinked structure as compared to flexible fluoro-carbon structure of Nafion[®] 117.

Table 3: Physical properties of the SPI/S-X membranes with different silica content

Polymer membranes	IEC (meq/g)		WU ^c (wt %)	λ^d [H ₂ O/SO ₃ ⁻]	Proton conductivity ^e (mS cm ⁻¹)		Oxygen permeability coefficient ^f (barrer)
	theo. ^a	exp. ^b			30 °C	90°C	
SPI/S-0	2.35	2.29	23.66	5.7	64.9	136.4	2.68
SPI/S-2.5	2.35	2.20	21.37	5.4	50.3	114.8	2.19
SPI/S-5	2.35	2.11	15.28	4.0	40.4	102.7	1.99
SPI/S-7.5	2.35	2.02	13.04	3.6	32	80.4	1.75
SPI/S-10	2.35	1.93	10.42	3.0	25.5	54.3	1.97
Nafion [®] 117*	-	0.95	18.52	10.83	62.8	150.1	3.58

^a Theoretically calculated (mmol of -SO₃H g⁻¹ + mmol of -COOH g⁻¹); ^b Measured by titration;

^c Measured at 30 °C; ^d Calculated by using experimental IEC value; ^e Measured in water;

^f Measured at 35 °C and 3.5 bar; 1 barrer = 10⁻¹⁰ cm³ (STP) cm/cm² s cm Hg.

* Values for Nafion have been measured in our test condition.

Proton conductivity and oxygen permeability. The proton conductivity of SPI/S-X membranes with different silica content was investigated as a function of temperature. The incorporation of the silica nanoparticles into the SPI polymer matrix is expected to influence the proton conductivity of the membrane. Also, the cross-linked network structure of the hybrid membranes played a significant role on proton conductivity. **Figure 9(a)** shows that at a fully hydrated measurement condition, the proton conductivities of both the pristine SPI membrane and hybrid SPI/S-X membranes increases as the temperature is increased from 30 to 90 °C. The proton conductivity of the hydrated membranes were found in the range of 25.5–64.9 mS/cm at 30 °C and 54.3–136.4 mS/cm at 90 °C and the values are listed in **Table 3**. Over the reported temperature range, the SPI/S-X hybrid membranes showed lower proton conductivity than the pristine SPI membrane. Similar observation was reported elsewhere.³¹ In addition, it was noticed that the proton conductivity of the hybrid membranes reduces with increasing of silica content at fully hydrated condition. Interestingly, when the proton conductivity of the membranes was tested at 75% RH condition it was noticed that the conductivity value increases with increasing of silica content up to 7.5 wt.% silica loading. Such enhancement of proton conductivity at relatively low humidity condition in the silica incorporated composite membrane was also reported in few recent studies.^{31,32} **Figure 9(b)** presented the change in proton conductivity of the SPI/S-X hybrid membranes under two different RH conditions at 30 °C.

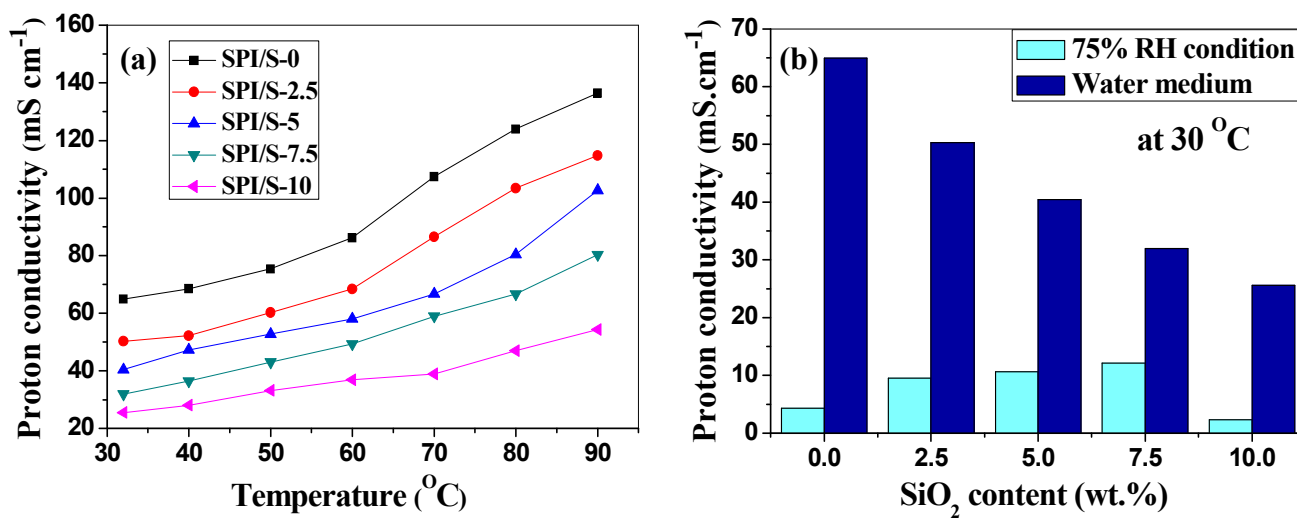


Figure 9. Change in proton conductivity of SPI/S-X membranes (a) at different temperature under fully hydrated condition (b) with different RH condition at 30 °C.

Generally, two types of mechanisms are used to describe the proton diffusion through the membrane. One is Grotthus (hopping) mechanism and the other is vehicle mechanism.³³ With increase in temperature, proton conductivity increases because the temperature strongly affects both mechanisms and the mobility of hydrated protons becomes faster under this condition. Now, with increase in silica content the lowering of proton conductivity of the membranes at fully hydrated condition is associated with the reduced WU values along with the dilution effect of silica on the sulfonic acid groups. However, at relatively low humidity (75 % RH) condition the state of water associated with SPI/silica hybrid membrane plays a vital role. The enhancement in proton conductivity with increasing of SiO₂ content at the low RH % is attributed to the presence of hygroscopic SiO₂ nanoparticles which can retain tightly bound water molecules in the SPI/S-X composite membranes. The hygroscopic Si-OH groups and cross-linking network also held some strongly bound water (i.e. chemically adsorbed water) that could compensate for the loss of free water to a certain degree. The bound water facilitated proton transport through the Grotthus mechanism, which contributed to enhancing the proton conductivity. This reveals that the incorporation of SiO₂ nanoparticles is beneficial to improve the proton conductivity at the low humidity condition. However, when SiO₂ content was increased to 10 wt.%, the proton conductivity of the hybrid membrane suddenly decreased. This is because, an excessive amount of SiO₂ particles in the membrane also causes agglomeration of the particles (supported by microstructural study), which blocks the hydrophilic pathways and

suppressed the transmission channel of hydrated protons. In this case, the bound water held by the hygroscopic $-\text{Si}-\text{OH}$ could not compensate the reduced IEC and loss of free water enough.³⁴

Activation energy (E_a) for proton conductivity of the SPI/S-X membranes was calculated from the plot of Arrhenius temperature dependent proton conductivity according to the Arrhenius equation:

$$\sigma = A \exp(-E_a/RT)$$

where, σ is the proton conductivity (mS/cm), A is the pre-exponential factor, R is the universal gas constant (8.314 J/mol K), and T is the absolute temperature (K).

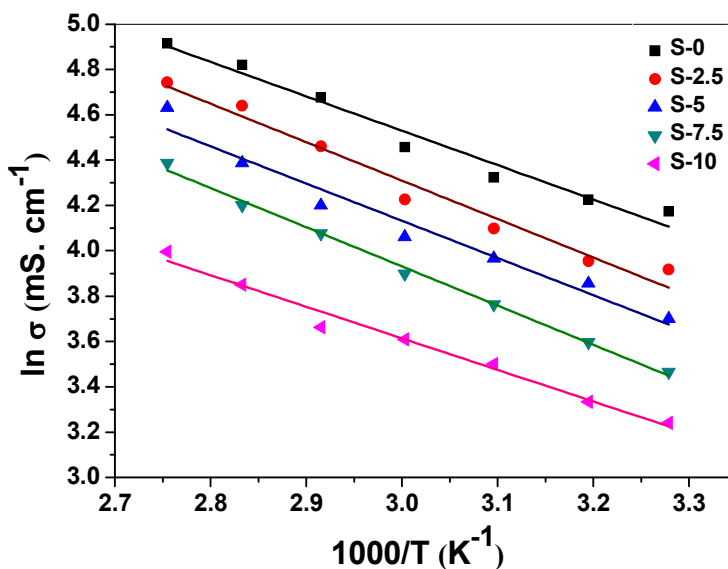


Figure 10. Arrhenius plot for the temperature dependent proton conductivity of SPI/S-X membranes.

Figure 10 depicted the Arrhenius temperature dependent plot for SPI/S-X membranes under fully hydrated condition. E_a is obtained from the slope at the linear fit of Arrhenius equation and it was found in the range 11.6–14.1 kJ/mol for SPI/S-X membranes. The E_a value of the hybrid membranes was found little higher than that of pristine SPI membrane. This can be explain by the fact that the nano-fillers acts as a carrier bridge for protons, hence little more energy is

required for proton transport. However, E_a for all the SPI/S-X membranes is close to Nafion[®] 117 (13.6 kJ/mol in our experimental condition) which indicates that similar to Nafion[®] 117, the prepared SPI/S-X membranes involved similar proton transport mechanism which resulted high proton conductivity in the range of Nafion[®] 117.

Despite lower IEC, Nafion[®] 117 has high proton conductivity due to strongly interconnected hydrophilic domain but it also possess high fuel crossover which is a serious drawback. Hybrid membrane with optimum filler loading may overcome this problem. The oxygen permeability coefficients (P_{O_2}) of Nafion[®] 117 and various SPI/S-X membranes were tested and the values are listed in **Table 3**. It can be seen from the table that the P_{O_2} of SPI and SPI-based hybrid membranes is less than that of Nafion[®] 117 ($P_{O_2} = 3.58$ barrer). Furthermore, the P_{O_2} decreases with increasing SiO₂ content for the hybrid membranes up to 7.5 wt.% filler loading ($P_{O_2} = 1.75$ barrer). It is well known that, oxygen molecules permeate through the membranes via a two-step mechanism, i.e. dissolving into the membrane and then diffusing through the membrane (solution-diffusion mechanism). The addition of SiO₂ nanoparticles can prevent the expansion of the membranes by forming a crosslinked network structure (as shown in **Figure 2**), and also block the transport channels of oxygen. As a result, oxygen permeability of the hybrid SPI/S-X membranes is lower than that of pristine SPI. However, addition of SiO₂ fillers does not proportionally reduce the P_{O_2} , but increases the oxygen crossover beyond a certain loading point. When the SiO₂ content is higher than 7.5 wt.% the particles started to get agglomerate to form clusters (as observed in the microstructure). It results the gap between the SPI inter-chains become bigger, which is helpful for the transportation of oxygen molecules. The P_{O_2} of SPI/S-10 increased to 1.97 barrer, but it is still lower than that of pristine SPI. The relatively low fuel (oxygen) crossover of the SPI/S-X membranes as compared to Nafion[®] 117 ($P_{O_2} = 3.58$ barrer),

indicating that the SPI-based hybrid membranes with optimum overall properties have potential to be used as proton exchange membrane for fuel cell application.

■ Conclusions

In this study, we report a simple and effective method for fabrication of sulfonated poly(ether imide)/silica hybrid electrolyte membranes for fuel cell application. Firstly, a fluorinated organo-soluble poly(ether imide) with active carboxyl pendant groups was successfully synthesized by polycondensation reaction using DSDSA, QA, DABA and NTDA. Thereafter, a series of hybrid nanocomposite membrane was prepared by reinforcing colloidal silica nanoparticles to the synthesized polymer matrix by solution mixing technique to have uniform dispersion of silica nanoparticles within the matrix. To enhance the compatibility between inorganic and organic phase, esterification reaction was carried out between the silanol (Si–OH) groups of colloidal silica and carboxyl (–COOH) groups present in the ter-copolymer by thermal treatment in the presence of *p*-toluenesulfonic acid as catalyst. This resulted in extensive crosslinking as was evident from the insoluble nature of thermally treated silica loaded hybrid membranes. The prepared hybrid membranes exhibited good thermal stability (~340 °C) which is much higher than servicing temperature (70 °C to 120 °C) for PEM fuel cell and superior mechanical property than that of pristine membrane and Nafion[®] 117. Mechanical properties of the hybrid membranes were enhanced (T.S up to ~95 M.Pa & Y.M up to 2.92 G.Pa) with certain wt.% of silica loading as compare to pristine SPI membrane. Swelling ratio of the hybrid membranes was reduced remarkably as compare to Nafion[®] and pristine SPI by introducing the cross-linked network structure which is considered as one of important parameter of the PEM to fabricate as membrane electrode assembly. Oxidative stability of the hybrid membranes increases significantly than that of pristine membrane and it showed an increasing trend with increasing silica content. Also the oxidative stability of the hybrid SPI/S-X

membranes was found much better than many other similar kind of membranes. Detailed morphological studies by various microscopic techniques confirmed the homogenous dispersion of silica nanoparticles in the hybrid membranes and the formation of well dispersed hydrophilic domain that results better PEM properties up to 7.5 wt.% of silica loading. However, excessive silica loading (10 wt.%) causes agglomeration of the particles which declines the physicochemical and PEM properties of membranes. The membranes exhibited high proton conductivity in water medium (up to 136.4 mS/cm at 90 °C) which is in the range of commercially available Nafion[®] membrane under the laboratory test condition. With increasing silica content proton conductivity of hybrid membranes reduced in water medium due to reduction of IEC and WU. On the contrary, an opposite trend was observed when the conductivity was measured at low humidity condition (75% RH) due to the presence of strongly bound water of silica particles that emphasize the advantageous effect of silica nanoparticles in the aspect of proton conductivity. The hybrid membranes also exhibited lower oxygen permeability (upto 51 %) as compare to Nafion[®] and the value reduced with increasing the amount of fillers. All these results suggested that such kind of hybrid SPI membranes containing cross-linked network structure has a potential application in PEMFCs.

Acknowledgements

E A Mistri thanks to Indian Institute of Technology, Kharagpur, India for the financial supports in the form of a Senior Research Fellowship (SRF) to carry out this work.

Notes and references

**Materials Science Centre, Indian Institute of Technology Kharagpur, Kharagpur-721302, India
Tel.: +91-3222-283972; fax: +91-3222-255303; E-mail: susanta@matsc.iitkgp.ernet.in*

† **Electronic Supplementary Information (ESI) available:** FT-IR spectra of the SPI/S-X membranes, ¹H-NMR spectrum of DDN-70 (model compound), Stress–strain plot of the SPI/S-X membranes, TEM images of the SPI/silica solution in DMSO.

References

- 1 Y. Wang, K. S. Chen, J. Mishler, S. C. Cho and X. C. Adroher, *Appl. Energy*, 2011, **88**, 981.
- 2 H. Zhang and P. K. Shen, *Chem. Rev.*, 2012, **112**, 2780.
- 3 A. Kusoglu, M. H. Santare and A. M. Karlsson, *J. Polym. Sci., Part B: Polym. Phys.*, 2011, **49**, 1506.
- 4 M. P. Rodgers, L. J. Bonville, H. R. Kunz, D. K. Slattery and J. M. Fenton, *Chem. Rev.*, 2012, **112**, 6075.
- 5 C. Wang, N. Li, D. W. Shin, S. Y. Lee, N. R. Kang, Y. M. Lee and M. D. Guiver, *Macromolecules*, 2011, **44**, 7296.
- 6 E. A. Weiber, S. Takamuku and P. Jannasch, *Macromolecules*, 2013, **46**, 3476.
- 7 J. Miyake, M. Watanabe and K. Miyatake, *ACS Appl. Mater. Interfaces*, 2013, **5**, 5903.
- 8 A. K. Mohanty, E. A. Mistri, S. Banerjee, H. Komber and B. Voit, *Ind. Eng. Chem. Res.*, 2013, **52**, 2772.
- 9 C. K. Shin, G. Maier and G. G. Scherer, *J. Membr. Sci.*, 2004, **245**, 163.
- 10 M. Linlin, A. K. Mishra, N. H. Kim and J. H. Lee, *J. Membr. Sci.*, 2012, **411–412**, 91.

- 11 C. Xu, Y. Cao, R. Kumar, X. Wu, X. Wang and K. Scott, *J. Mater. Chem.*, 2011, **21**, 11359.
- 12 K. Yamazaki and H. Kawakami, *Macromolecules*, 2010, **43**, 7185.
- 13 C. Liu, L. Li, Z. Liu, M. Guo, L. Jing, B. Liu, Z. Jiang, T. Matsumoto and M. D. Guiver, *J. Membr. Sci.*, 2011, **366**, 73.
- 14 E. A. Mistri, A. K. Mohanty, S. Banerjee, H. Komber and B. Voit, *J. Membr. Sci.*, 2013, **441**, 168.
- 15 B. R. Einsla, Y. T. Hong, Y. S. Kim, F. Wang, N. Gunduz and J. E. McGrath, *J. Polym. Sci., Part A: Polym. Chem.*, 2004, **42**, 862.
- 16 R. Souzy and B. Ameduri, *Prog. Polym. Sci.*, 2005, **30**, 644.
- 17 F. Sun, T. Wang, S. Yang and L. Fan, *Polymer*, 2010, **51**, 3887.
- 18 H. Pan, H. Pu, D. Wan, M. Jin and Z. Chang, *J. Power Sour.*, 2010, **195**, 3077.
- 19 D. Liu, L. Geng, Y. Fu, X. Dai and C. Lü, *J. Membr. Sci.*, 2011, **366**, 251.
- 20 K. Vanherck, G. Koeckelberghs and I. F.J. Vankelecom, *Prog. Polym. Sci.*, 2013, **38**, 874.
- 21 H. B. Park, C. H. Lee, J. Y. Sohn, Y. M. Lee, B. D. Freeman and H. J. Kim, *J. Membr. Sci.*, 2006, **285**, 432.
- 22 A. K. Mishra, S. Bose, T. Kuila, N. H. Kim and J. H. Lee, *Prog. Polym. Sci.*, 2012, **37**, 842.
- 23 C. H. Lee, S. Y. Hwang, J. Y. Sohn, H. B. Park, J. Y. Kim and Y. M. Lee, *J. Power Sour.*, 2006, **163**, 339.
- 24 S. Banerjee, M. K. Madhra, A. K. Salunke and D. K. Jaiswal, *Polymer*, 2003, **44**, 613.
- 25 F. Wang, M. Hickner, Y. S. Kim, T. A. Zawodzinski and J. E. McGrath, *J. Membr. Sci.*, 2002, **197**, 231.

- 26 S. Sen, B. Dasgupta, S. Banerjee, *J. Membr. Sci.* 2009, **343**, 97.
- 27 J. H. Chun, S. G. Kim, J. Y. Lee, D. H. Hyeon, B. H. Chun, S. H. Kim and K. T. Park, *Renew. Energy*, 2013, **51**, 22.
- 28 S. Y. Lee, N. R. Kang, D. W. Shin, C. H. Lee, K. S. Lee, M. D. Guiver, N. Li and Y. M. Lee, *Energy Environ. Sci.*, 2012, **5**, 9795.
- 29 L. Zou, S. Roddecha and M. Anthamatten, *Polymer*, 2009, **50**, 3136.
- 30 N. Asano, M. Aoki, S. Suzuki, K. Miyatake, H. Uchida and M. Watanabe, *J. Am. Chem. Soc.*, 2006, **128**, 1762.
- 31 J. H. Won, H. J. Lee, K. S. Yoon, Y. T. Hong and S. Y. Lee, *Int. J. Hydr. Energy*, 2012, **37**, 9202.
- 32 J. R. Lee, J. H. Won, N. Y. Kim, M. S. Lee and S. Y. Lee, *J. Colloid Interface Sci.*, 2011, **362**, 607.
- 33 S. J. Peighambardoust, S. Rowshanzamir and M. Amjadi, *Int. J. Hydr. Energy*, 2010, **35**, 9349.
- 34 J. Ren, S. Zhang, Y. Liu, Y. Wang, J. Pang, Q. Wang and G. Wang, *J. Membr. Sci.*, 2013, **434**, 161.

Scheme and Figures legends

Scheme 1. Synthetic procedure of fluorine-containing SPI with reactive carboxyl groups.

Figure 1. $^1\text{H-NMR}$ spectrum of DQDN-70 copolymer with signal assignment.

Figure 2. Cross-linked structure of SPI/silica hybrid membrane.

Figure 3. Solubility of SPI/S-X membranes in DMAc solvent.

Figure 4. EDS spectra of (a) pristine SPI and (b) SPI/S-2.5

Figure 5. Thermogravimetric analysis of SPI/S-X hybrid membranes (a) thermograms of the representative samples; (b) correlation plot of SiO_2 feed versus residual mass in wt.%

Figure 6. Dimensional swelling of SPI/S-X membranes and Nafion[®] 117 at 30 °C.

Figure 7. SEM images of the membrane surface with different SiO_2 contents (a) SPI/S-0; (b) SPI/S-2.5; (c) SPI/S-7.5; (d) SPI/S-10.

Figure 8. TEM images of SPI/S-X membranes (a) SPI/S-0; (b) SPI/S-2.5; (c) SPI/S-5; (d) SPI/S-7.5; (e) SPI/S-10 (cross section, in Ag^+ form).

Figure 9. Change in proton conductivity of SPI/S-X membranes (a) at different temperature under fully hydrated condition (b) with different RH condition at 30 °C.

Figure 10. Arrhenius plot for the temperature dependent proton conductivity of SPI/S-X membranes.

Tables

Table 1. Mechanical properties of different hybrid membranes

Table 2. Oxidative stability and dimensional stability of SPI/S-X membranes

Table 3: Physical properties of the SPI/S-X membranes with different silica content